AMERICAN COLLEGE OF
PROSTHODONTISTS
Your smile. Our specialty.®

Fracture strength of monolithic and glass-soldered ceramic subcomponents of 5-unit fixed dental prosthesis

Jan-Oliver Sass MSc[1,2] | Ulrike Burmeister Dr Med Dent[2] | Cornelia Ganz Dr Rer Nat[3] | Aurica Mitrovic[3] | Hermann Lang Dr Med Dent[2] | Rainer Bader Dr Med DipIng[1] | Danny Vogel MSc[1]

[1]Department of Orthopedics, Rostock University Medical Center, Rostock, Germany

[2]Department of Operative Dentistry and Periodontology, Rostock University Medical Center, Rostock, Germany

[3]ZM Präzisionsdentaltechnik GmbH, Rostock, Germany

Correspondence
Jan-Oliver Sass, MSc, Department of Orthopedics, Rostock University Medical Center,Doberaner Straße 142, 18057 Rostock, Germany.
Email: jan-oliver.sass@med.uni-rostock.de

Abstract

Purpose: Zirconium dioxide ceramic has been successfully introduced as a framework material for fixed dental prostheses. To reduce manufacturing constraints, joining of subcomponents could be a promising approach to increase the mechanical performance of long-span fixed dental prostheses. In this experimental study, the biomechanical behavior of monolithic and soldered framework specimens for fixed dental prostheses made of Y-TZP was investigated.

Materials and methods: Framework specimens (n = 80) of 5-unit fixed prostheses made of Y-TZP were prepared and divided into 10 equal groups. The specimens were monolithic or composed of subcomponents, which were joined using a silicate-based glass solder. Thereby, three joint geometries (diagonal, vertical with an occlusal cap, and dental attachment-based) were investigated. Moreover, the groups differed based on the mechanical test (static vs. dynamic) and further processing (veneered vs. unveneered). The framework specimens were cemented on alumina-based jaw models, where the canine and second molar were acting as abutments before a point-load was applied. In addition, μCT scans and microscopic fractography were used to evaluate the quality of soldered joints and to determine the causes of fracture.

Results: The determined fracture loads of the different unveneered framework specimens in static testing did not vary significantly ($p = 1$). Adding a veneering layer significantly increased the mechanical strength for monolithic framework specimens from 1196.29 ± 203.79 N to 1606.85 ± 128.49 N ($p = 0.008$). In case of soldered specimens with a dental attachment-based geometry, the mechanical strength increased from 1159.42 ± 85.65 N to 1249.53 ± 191.55 N ($p = 1$). Within the dynamic testing, no differences were observed between monolithic and soldered framework specimens. μCT scans and fractography proved that the dental attachment-based joining geometry offers the highest quality.

Conclusion: Using glass soldering technology, subcomponents of 5-unit framework specimens made of Y-TZP could be joined with mechanical properties comparable to those of monolithic frameworks.

KEYWORDS
Y-TZP, dental restoration, 5-unit fixed dental prosthesis, glass soldering

The superior physical, biological, aesthetic, and corrosion properties of yttria-tetragonal zirconia polycrystal (Y-TZP) compared to commonly used metals and their alloys, offer promising optimization of implants and restorations for dentistry.[1] Stress-induced tetragonal to monoclinic phase martensitic transformation of Y-TZP leads to high fracture toughness.[2] Thus, Y-TZP has been successfully introduced as a framework material for fixed dental prosthesis (FDP)[3,4] and no significant differences have been found between Y-TZP FDP and metal-ceramic FDP in terms of biological and technical complications.[5] Since some components in the typically used metal alloys have been shown to have cytotoxic and allergic effects in vitro, if the concentration exceeds patient individual limits[6,7], it is assumed that increasing numbers of Y-TZP-based FDP will be implanted in the future.[8,9]

Three-unit FDP composed of Y-TZP has been shown to have high survival rates of 98.1%, 95.5%, and 91.0% after 5, 11, and 14 years, respectively.[3,4,10] However, fracture risk increases with the number of bridged teeth and in relation to the location in the jaw.[11,12] Schmitter et al[12] have reported a survival rate of long-span (more than four artificial teeth) monolithic zirconia FDP of 82% after 5 years, which is substantially lower than the survival rate of three-unit FDP.[3]

Bridging large spans of teeth with healthy periodontium is restricted by manufacturing constraints as the manufacture of FDP requires pre-sintering, soft machining of a green body, sintering, and hard machining of the fully sintered ceramic, in combination with final veneering or surface finish. These production techniques are associated with the formation of flaws and residual stresses, which decrease mechanical strength.[13]

Furthermore, linear shrinkage (20-25%) during sintering is dependent on the specific geometrical shape and manufacturing process of the Y-TZP blanks.[14,15] The shrinkage causes warpage, which may increase with the length and complexity of the FDP.[13,16] This warpage induces further residual stresses and enhances marginal misfit, whereby the risk of failure increases.[14,16]

Manufacturing smaller subcomponents and joining these is a feasible approach to overcoming the limitations of decreased fit and distortions during the sintering of long-span FDP.[17–19]

Wimmer et al[17] investigated approaches to joining ceramic-based FDP in order to improve the marginal fit and mechanical strength of four-unit FDP. They found that the mechanical strength was within the range of monolithic FDP, but no fatigue testing was performed. The silicate-based glass solder used in this study has shown promising results.[17]

In a recent study, Sass et al[20] described a manufacturing method for the sufficient joining of Y-TZP subcomponents, which can be performed using the standard equipment of a dental laboratory and a silicate-based glass solder. However, the investigation was restricted to rectangular bars and no complex-shaped parts have been joined with the described method yet.

This experimental study aimed to investigate the applicability of the glass soldering technology to join complex-shaped subcomponents of 5-unit FDP made of Y-TZP with high mechanical strength for use in the highly demanding biomechanical environment. Therefore, framework specimens of long-span 5-unit FDP, bridging the premolars and the first molar in the maxilla using the canine and second molar as terminal abutments, were manufactured with three different joint geometries. Monolithic framework specimens were used as references. In addition, the influence of the veneering was investigated for both the monolithic and best-performing soldered framework specimens. Static and dynamic three-point bending tests in combination with μCT analysis and fractography were carried out.

The null hypotheses were: (1) glass soldering technology is applicable to join subcomponents made of Y-TZP with sufficient mechanical strength and (2) the joining geometry has no influence on the mechanical strength of soldered framework specimens.

MATERIALS AND METHODS

Master model

A master model was established to produce standardized framework specimens. Therefore, a duplicating mold of the teeth of interest was filled with gypsum. This model was scanned and reconstructed using 3Shape Dental System Version 2018 (3Shape, Copenhagen, Denmark).

Preparation of framework specimens

Five-unit framework specimens (n = 80) were milled from pre-sintered Y-TZP (stabilized with 6.9 wt% yttria) blocks (Z-CAD® One4All Multi, Metoxit GmbH, Thayngen, Switzerland) using a 5-axis milling machine (Desktop 8, R+K CAD/CAM Technologies GmbH & Co. KG, Berlin, Germany) and subsequently sintered at 1500°C. The connector dimensions were set to 4×4 mm^2 and the framework specimens were designed to bridge the premolars and the first molar in the maxilla. The canine and second molar were thus acting as terminal abutments.

The framework specimens were divided into 10 groups, which are specified in Table 1. Figure 1 shows the general procedure of the study. The sample size of 8 for each group was based on preliminary studies.[11,21]

The investigated joint geometries (diagonal, vertical with an occlusal cap, and dental attachment-based) are shown in Figure 2. The diagonal joint geometry was made by separating monolithic framework specimens with a cutting disk. The other two joint geometries were designed in 3Shape Dental System Version 2018 (3Shape, Copenhagen, Denmark) using library templates as starting points. These templates were modified for the specific requirements of the Y-TZP-based subcomponents and were also milled from pre-sintered Y-TZP blocks.

The joint geometries were selected by experienced dental technicians as well as experts in glass soldering of

TABLE 1   Description of the investigated groups

Group*	Framework specification		Mechanical test
1	Monolithic	Unveneered	Quasi-static
2	Soldered, diagonal joint geometry		
3	Soldered, vertical joint geometry with an occlusal cap		
4	Soldered, dental attachment-based joint geometry		
5	Monolithic	Veneered	
6	Soldered, dental attachment-based joint geometry		
7	Monolithic	Unveneered	Dynamic
8	Soldered, diagonal joint geometry		
9	Soldered, vertical joint geometry with an occlusal cap		
10	Soldered, dental attachment-based joint geometry		

*Each group consisted of n = 8 framework specimens.
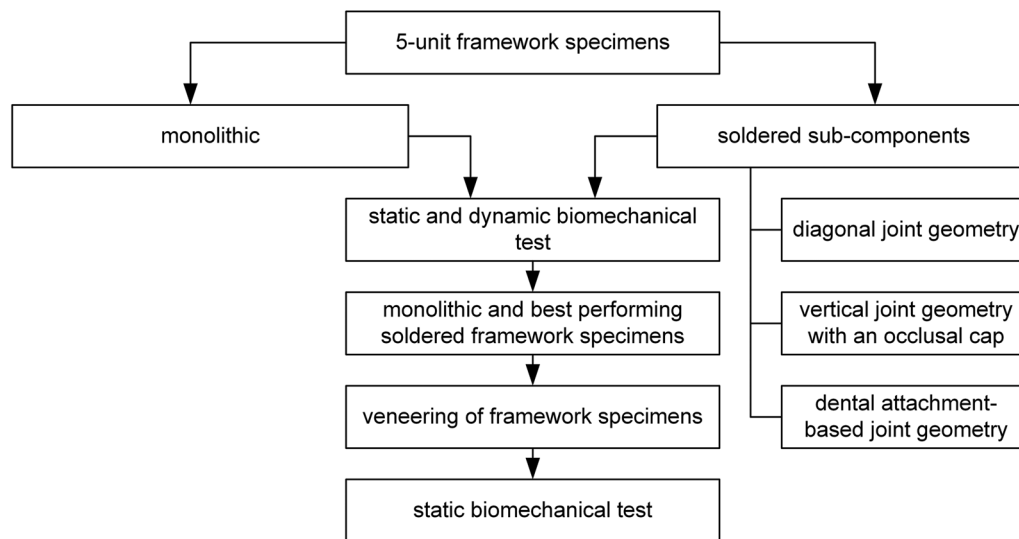
FIGURE 1   Flowchart of the study to investigate the static and dynamic mechanical behavior of monolithic and soldered 5-unit framework specimens.

dental ceramics. The diagonal geometry and the vertical joint geometry with an occlusal cap were developed as extensions of the work of Wimmer et al,[17] where monolithic frameworks were separated perpendicularly. Compared to this joint geometry, those of the present study have the advantage of an increased cross-section at the soldered joint. The dental attachment-based geometry was adopted from other attachments, which are frequently used in dental prostheses, for example, ERA attachments (Sterngold Co., Attleboro, MA). The specific design was customized to ensure the milling production and soldering. The male and female parts of the dental attachment-based subcomponents formed a defined joint gap.

Selected framework specimens were veneered using Cercon® Ceram Kiss (DeguDent GmbH, Hanau, Germany) according to the instruction guidelines (layering technique) and subsequently were statically tested as well. The selection was based on the static tests of unveneered framework specimens.

The manufacturing process for the glass-soldered joint was adopted from a previous study and consisted of surface preparation, cleaning, and soldering.[20] Within that study by Sass et al,[20] the influence of different surface treatments and ambient conditions on the soldered joint of rectangular specimens was investigated. Therefore, in this study, the joint surfaces were cleaned in an ultrasonic bath with ethanol and subsequently stored in ethanol for 30 minutes. The subcomponents were mounted on a jaw model (canine and second molar as abutment) made of firing pillow. The gap between the subcomponents was filled with highly viscous glass solder paste. This paste was produced by blending the glass solder powder with Duceram Plus SMH-Liquid (DeguDent GmbH, Hanau, Germany). The silicate-based glass solder consisted of SiO_2, Al_2O_3, K_2O, Na_2O, SrO, ZnO, SnO_2, CeO_2, and La_2O_3. To reduce air voids in the joint, the framework specimens were set under a pressure of 2 bar in a dental pressure pot until the paste was solidified. The furnace soldering was performed with a heating and cooling rate of 55 K $\times$ min^{-1}
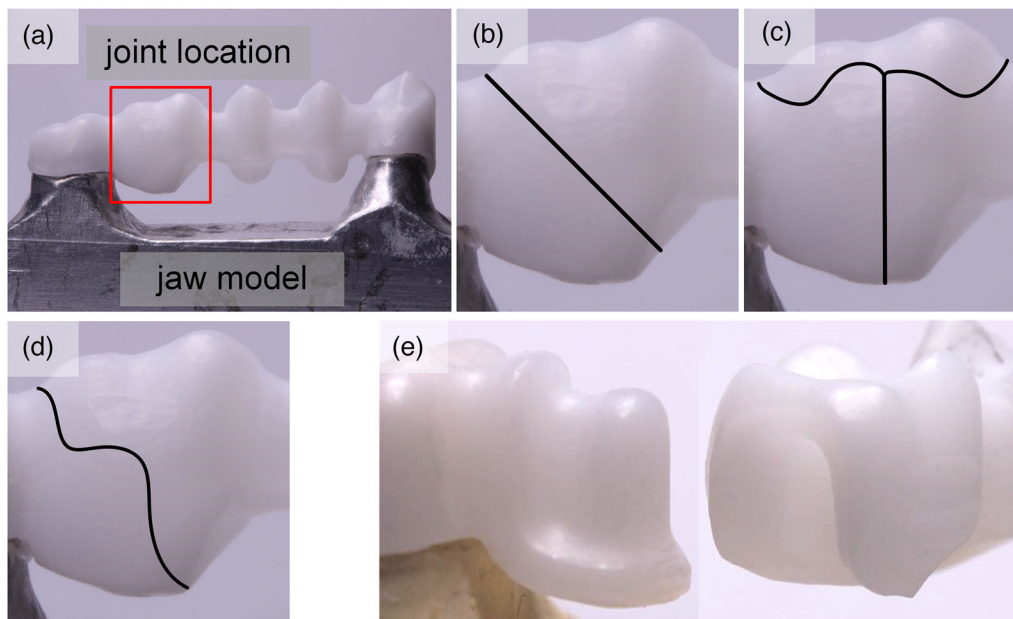
FIGURE 2 Schematic presentation of the investigated joint geometries for the soldered subcomponents: (a) location of the joint, (b) diagonal joint geometry, (c) vertical joint geometry with an occlusal cap, (d) dental attachment-based joint geometry, and (e) male (left) and female (right) part of the attachment-based subcomponents.

and the maximum temperature of 950°C was held for 1 minute.

The coefficients of thermal expansion (CTE) of the materials used were $9.5 \times 10^{-6} \text{ K}^{-1}$ (glass solder), $10.0 \times 10^{-6} \text{ K}^{-1}$ (veneering ceramic), and $10.5 \times 10^{-6} \text{ K}^{-1}$ (Y-TZP).

For the quality assessment of the soldered joints, μCT scans were taken (Skyscan1076, Bruker, Billerica, MA) with a voxel edge length of 18.44 μm. The voltage and current were set to 95 kV and 104 μA, and a 0.5 mm aluminum filter was used. All scanned framework specimens were analyzed in Amira 5.4.1(Thermo Fisher Scientific, Waltham, MA) to determine any visible air voids and misalignment of the subcomponents.

Biomechanical testing and fracture analysis

The biomechanical properties of the framework specimens were evaluated in static and dynamic tests, with a point-load on the central fossa of the second premolar mimicking a worst-case scenario. A stainless-steel cylinder (Ø 3 mm) and a 0.2 mm thick tin foil was used as load indentation to ensure an even stress distribution and to avoid stress peaks in the ceramic. Therefore, the test setup in this study based on patient-specific contacts of the occlusal surface with hard food objects (e.g., nuts, seeds, and errant particulates) in the mm-scale[22] and is comparable to a three-point-bending test, which is frequently used to investigate FDP.[11,23–25] All tests were performed with a shear force bearing.
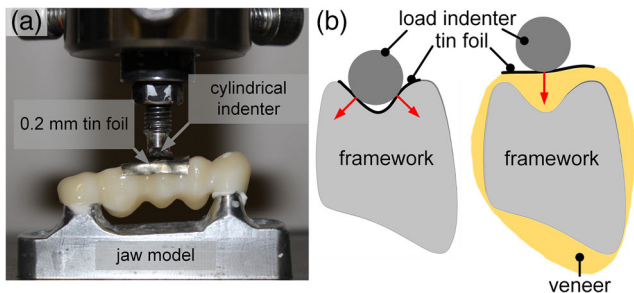
Before the biomechanical tests, the framework specimens were cemented on simplified jaw models (one model for each group) using zinc-phosphate cement (Harvard Cement, Harvard Dental International GmbH, Hoppegarten, Germany). The jaw models and abutment teeth were made of aluminum and simulated the maxilla, where the canine and second molar are acting as abutments. The premolars and the first molar were bridged with the manufactured framework specimens. The jaw models with the two abutment teeth were CNC-machined from an aluminum block and were based on the master model. The surface reduction of the abutment teeth was based on two principles: the least possible surface reduction and secondly a minimum wall thickness of 0.5 to 0.7 mm (instruction guideline).

The framework specimens were statically loaded until fracture (crosshead speed: 1 mm × min $^{-1}$) in a universal testing machine (Zwick Roell Z050-50 kN, Zwick Roell, Ulm, Germany). Figure 3 shows the static test setup and the different contact conditions at the second premolar with the load indenter of both the unveneered and veneered framework specimens.

The dynamic tests were performed with an electro-dynamic testing machine (Zwick Roell LTM5, Zwick Roell, Ulm, Germany) referring to the standard ISO 14801:2016.[26] The specimens were sinusoidally loaded for 2 million cycles in deionized water with a constant temperature of 37°C and a frequency of 2 Hz. The load ratio R was set to 0.1.

The fatigue tests were carried out with different load levels between maximum forces of 600 and 900 N. 900 N was set as the maximum value and represents approximately 75% of the average static fracture load of all the unveneered framework specimens. Since no comparable studies were available, a wide span of maximum loads was tested to determine a range

FRACTURE STRENGTH OF MONOLITHIC AND GLASS-SOLDERED CERAMIC SUBCOMPONENT

AMERICAN COLLEGE OF
PROSTHODONTISTS
Your smile. Our specialty.®

5

FIGURE 3 Illustration of (a) the static biomechanical test set-up with a Y-TZP based veneered framework specimen and (b) the principal contact between the load indenter (∅3 mm cylinder) and the unveneered (left) and veneered framework specimen (right), respectively, where the induced compressive forces are schematically indicated with a red arrow.

TABLE 2 Load levels of the dynamic staircase test (minimum, maximum and mean values in N) and sample size for each individual test with a constant frequency of 2 Hz and a stress ration R = 0.1

| Minimum load [N]	Maximum load [N]	Mean load [N]	Sample size
90.0	900.0	495.0	4
75.0	750.0	412.5	1
67.5	675.0	371.3	2
60.0	600.0	330.0	1

where the specimens conform to the defined specifications in the standard ISO 14801:2016.[26]

First, 4 specimens of each group were tested at a high maximum load of 900 N. Afterwards, a staircase test was performed with a step width of 75 N starting at a maximum load of 750 N. The loading regimes used and the number of tested specimens are summarized in Table 2. Framework specimens surviving 2 million cycles were loaded until fracture with the static loading protocol to investigate the remaining mechanical strength.

The fracture analyses were performed in line with a recommended practice guide for fractography of ceramics and glasses[27] using a digital microscope (VHX-6000, Keyence Corporation, Osaka, Japan). All fractured specimens were examined to determine the origin and cause of the fracture.

Statistical analysis

The statistical analysis was performed in SPSS Statistics (v25, IBM Corp., Armonk, NY) and the level of significance was $p < 0.05$ for all tests. The static fracture loads were tested for normal distribution using the Shapiro-Wilk test, for variance homogeneity using Levene's test, and for significant differences with a one-way ANOVA together with the Bonferroni post-hoc test. Since the fatigue tests are limited to n = 8 specimens for each group and they were tested with different load levels, no statistical analysis was appropriate and only the descriptive statistics are specified.
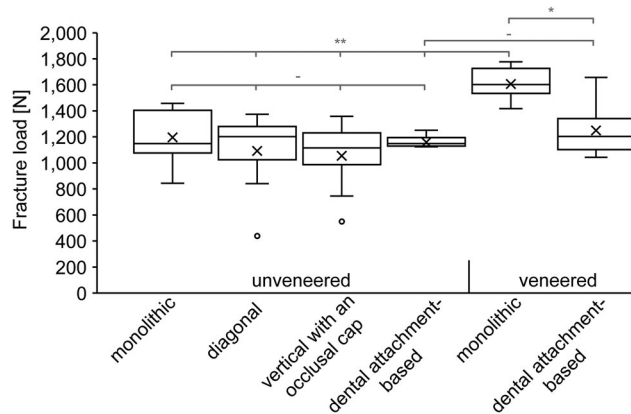
FIGURE 4 Boxplots (mean value, standard deviation, median, minimum, maximum, outliers) of the static fracture strengths in N of the monolithic and the soldered framework specimens with a diagonal joint geometry, a vertical joint geometry with an occlusal cap, and a dental attachment-based joint geometry. Significant differences (Bonferroni post-hoc test) are indicated: $p \geq 0.05$ (–), $p < 0.05$ (*), and $p < 0.01$ (**).
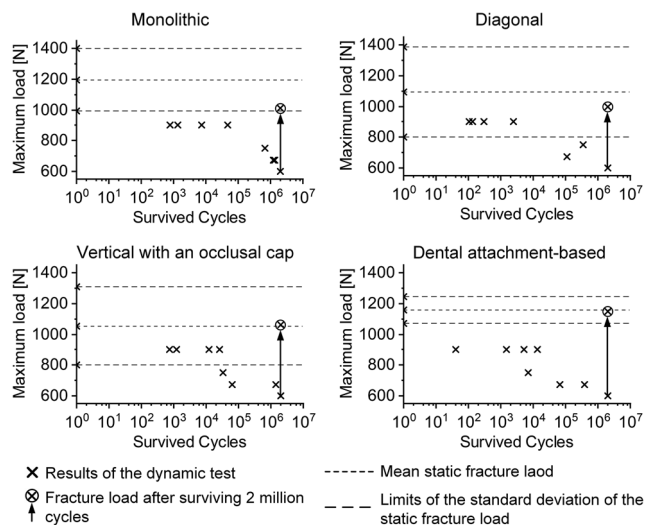
RESULTS

The static fracture load was normally distributed for all groups ($p > 0.05$), with homogeneous variance ($p = 0.130$). The level of significance for the Shapiro-Wilk tests ranged from $p = 0.071$ (unveneered, diagonal) to $p = 0.605$ (unveneered, dental attachment-based). According to the one-way ANOVA, the fracture strength was significantly different between groups ($p < 0.001$).

Based on the post hoc test, no significant differences were found between unveneered monolithic and glass-soldered framework specimens. However, the monolithic veneered framework specimens had a significantly higher fracture load than the unveneered monolithic ($p = 0.008$) and veneered glass-soldered specimens with a joint geometry based on a dental attachment ($p = 0.033$). The descriptive statistics of the static tests and results of the post hoc test are shown in Figure 4. For soldered framework specimens outliers were identified, which were associated with fracture within the soldered joint. The mean and standard deviation were as follows: 1196.29 ± 203.79 N (unveneered, monolithic), 1092.36 ± 292.19 N (unveneered, diagonal), 1054.45 ± 252.24 N (unveneered, vertical with occlusal cap), 1159.42 ± 85.65 N (unveneered, dental attachment), 1606.85 ± 128.49 N (veneered, monolithic), and 1249.49 ± 191.55 N (veneered, dental attachment).

The dynamic tests showed that, for all groups, the framework specimens survived 2 cycles with a maximum load of 600 N. For the other loading regimes, a wide range of cycles were observed until fracture and no clear trends were found between groups. In Figure 5, the results of the dynamic tests are plotted in load-life diagrams. For the group with a diagonal joint geometry one specimen fractured during handling and preparation for the test.

The remaining strength of the framework specimens that survived 2 million cycles (one per group), was in the range

Monolithic — Maximum load [N] vs Survived Cycles

Diagonal — Maximum load [N] vs Survived Cycles

Vertical with an occlusal cap — Maximum load [N] vs Survived Cycles

Dental attachment-based — Maximum load [N] vs Survived Cycles

× Results of the dynamic test

⊗↑ Fracture load after surviving 2 million cycles

------ Mean static fracture laod

_ _ _ Limits of the standard deviation of the static fracture load

FIGURE 5 Load-life diagrams (maximum load in N and survived cycles) of dynamically tested unveneered framework specimens, the mean static fracture load, the lower and upper limit of the standard deviation, and the remaining mechanical strength after surviving 2 million cycles (the limit described in the standard ISO 14801:201626) for the monolithic and glass-soldered framework specimens.

of the results of the static tests. Fracture loads of 1019.17 N (monolithic), 999.43 N (diagonal), 1059.01 N (vertical with an occlusal cap), and 1154.46 N (dental attachment) were measured.

The μCT analysis and fractography revealed the specific causes of fracture. In general, the fracture occurred within the soldered joint (n = 3) or at the second premolar (n = 77), where the load was applied.

The μCT analysis showed that all framework specimens that fractured at the soldered joint were influenced by manufacturing-related defects (Fig 6). This fracture mode was observed in 1 framework specimen with a diagonal joint geometry (fracture load: 439.01 N) and in 2 with a vertical joint geometry with an occlusal cap (fracture load: 745.02 N and 550.22 N). All joint failures occurred during static testing of unveneered framework specimens. The fracture surfaces showed a mixed mode of adhesive and cohesive failure.

The soldered framework specimens with a dental attachment-based joint geometry showed a high quality in terms of air voids and alignment of the subcomponents and a homogeneous layer of glass solder in the μCT scans.

Based on microscopic fractography, the failure around the second premolar can be divided into three fracture patterns: fracture in the connector region, fracture in the dental cusp of the second premolar with splitting of the tooth, and chipping of the veneer. The fracture patterns were also observed in combination. Figure 7 shows the different fracture surfaces of unveneered and veneered frameworks specimens after static and dynamic tests.

The fracture in the connector region began on the gingival side, where tensile stresses are induced and the cross-section is minimal. Furthermore, subsurface cracking was observed to be occlusal, where the load was transferred and compres-

sive forces are induced. Lateral (lingual or buccal) splitting of the second premolar was observed to originate from the occlusal cracking zone.

The occlusal surface and contact area with the load indenter of the veneered framework specimens are characterized by an extensive cracking zone. Chipping of the ceramic veneer and the Y-TZP was observed. Fracture of the veneered framework specimens always occurred in the connector region and no splitting of the second premolar occurred. No differences were observed between the monolithic and glass-soldered framework specimens.

During the dynamic tests, all specimens fractured due to the splitting of the second premolar. Extensive subsurface cracking was observed in the occlusal surface.

DISCUSSION

Manufacturing of zirconia-based long-span FDP is limited due to the formation of residual stresses during processing[13–17] and joining of smaller subcomponents is a feasible approach to overcome this limitation.[17–19] Therefore, this experimental study investigated the biomechanical behavior of Y-TZP-based 5-unit framework specimens. These were monolithic or composed of subcomponents, which were joined using a silicate-based glass solder. Three joint geometries were introduced: diagonal joint geometry, vertical joint geometry with an occlusal cap, and a dental attachment-based joint geometry. The preparation of the joint was done with standard equipment of a dental laboratory and according to a previously published method for joining Y-TZP.[20]

Several studies have investigated the mechanical strength of three-unit FDP[11,25,28–30] and four-unit FDP.[17,31] To the best of the author's knowledge, no experimental study has been performed with Y-TZP based 5-unit FDP. Therefore, the comparison of the present results to other studies is limited. In the literature, fracture loads of veneered three-unit zirconia frameworks ranged from 659 ± 182 N[23] to 3291 ± 444 N[30] and, for veneered four-unit zirconia frameworks, from 405 ± 112 N[11] to 1021.6 ± 253.8 N[31] after simulating mechanical and thermal aging. The approach of joining ceramic-based framework specimens using the glass soldering technology was previously investigated with veneered four-unit zirconia frameworks. In this study, the soldered framework specimens showed a fracture load of 1132 ± 490 N without applying simulated aging.[17]

Therefore, the static fracture strengths determined in this study were in the range of previously-described results of smaller veneered framework specimens.[11,17,23,31] However, the fracture loads of three-unit framework specimens reported by Sundh et al[30] are higher than those of the present study, which is probably due to the increased length.

Whether the fracture load of framework specimens is sufficient has to be evaluated with respect to physiological loads occurring in vivo. The maximum bite forces in humans are described for the molar region.[32–34] Padma et al[33]

AMERICAN COLLEGE OF
PROSTHODONTISTS | 7
Your smile. Our specialty.®
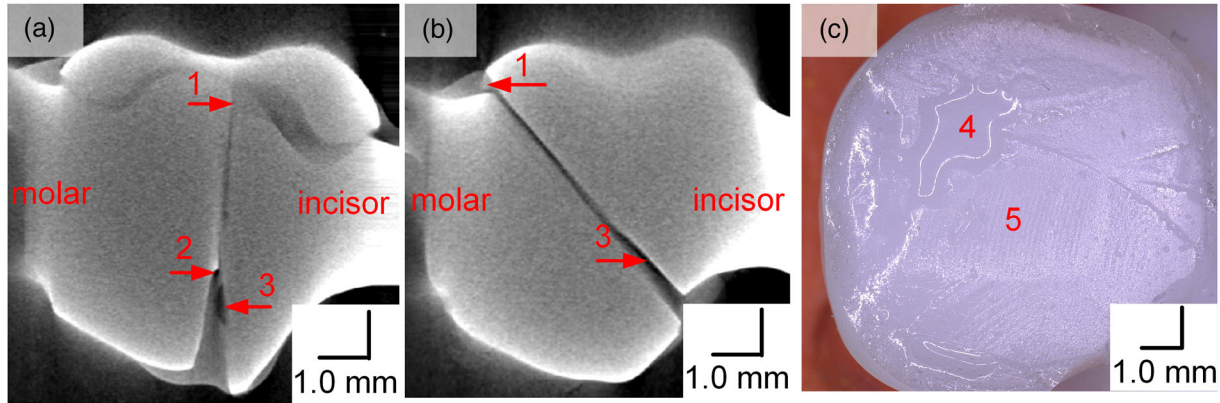
FIGURE 6 Fracture pattern of framework specimens that fractured in the glass-soldered joint showing μCT images of specimens with (a) a vertical joint geometry with an occlusal cap, (b) a diagonal joint geometry, and (c) a microscopic image of the fracture surface of the specimen shown in (b), indicating 1: shift of the subcomponents and misalignment, 2: discontinuous joint surface, 3: air inclusion, 4: region of adhesive failure, and 5: region of cohesive failure.
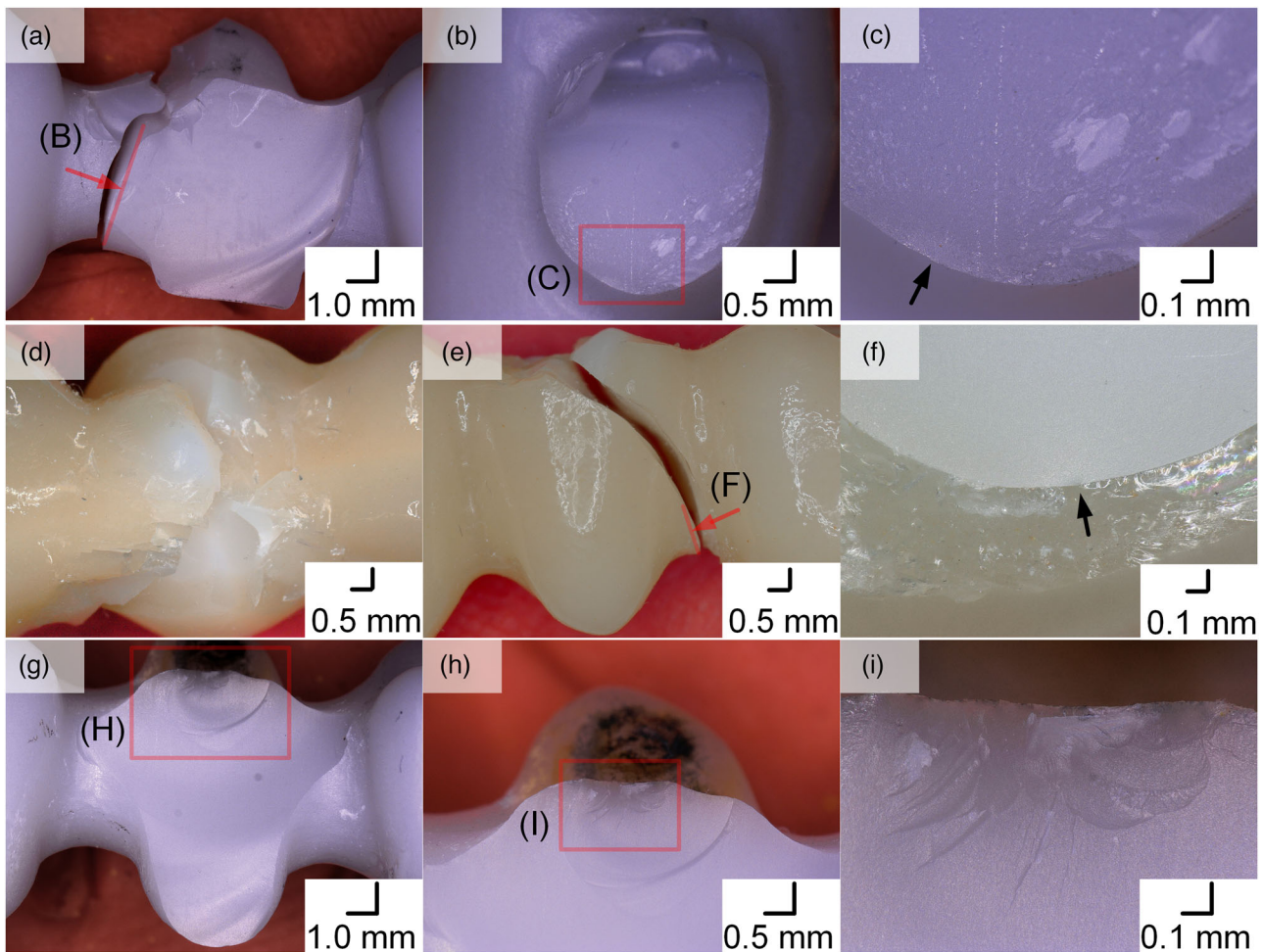
FIGURE 7 Fractographic images of tested specimens and detailed presentation of the region around the second premolar; top (unveneered, monolithic framework, static fracture test): (a) lateral view of the fracture surface characterized by fracture in the connector region and splitting of the tooth, (b) sagittal view of the fracture surface, (c) indication of the fracture origin at the gingival side; middle (veneered, monolithic framework, static fracture test): (d) occlusal surface, (e) lateral view of the fracture surface, characterized by fracture in the connector region and formation of a compression curl, (f) indication of the fracture origin in the framework; bottom (unveneered, monolithic framework specimen, dynamic test for 2 million cycles with a maximum load of 600 N, followed by a static fracture test): (g) lateral fracture surface, characterized by splitting of the tooth, (h) lateral view of the occlusal surface in the region of the load transfer, and (i) coronal subsurface cracking due to compressive forces.

reported a range of 475 N to 752 N for the molar region, 269 N to 475 N in the premolar region, and 182 N to 350 N in the incisor region, and Bakke et al[32] confirmed those loads (range: 300-600 N). However, in another study, Cosme et al[34] reported higher maximum bite forces up to 1.009 ± 290 N for m and 668 ± 179 N for female adults. Furthermore, Rodriguez et al[35] reported that biting forces can reach up to 1000 N under parafunctional habits. In comparable experimental studies, it was reasonable to assume that a static fracture load of 1000 N is sufficient for initial fracture resistance.[36]

The fracture load of all the tested groups was in the range of the maximum reported biting forces, however, the clinical acceptance should be comprehensively investigated in clinical situations.[36] Since manufacturing defects might lead to fracture within the soldered joint under lower loads, a high-quality standard is necessary and any voids or misalignment must be avoided.

The fracture load of the framework specimens showed no significant difference, whether they were monolithic or joined, which indicates the feasibility of the glass-soldering technology to join Y-TZP subcomponents with sufficient mechanical strength. The veneered monolithic framework specimens showed the highest fracture load in static test conditions, with a significant difference as compared to the unveneered monolithic framework specimens. The increase in fracture load can be explained by various effects, e.g., phase transformation in Y-TZP, change in grain size during any kind of heat treatment,[30] relaxation of the surface compressive forces that were formed during the machining process,[37] infiltration of defects on the surface of Y-TZP framework specimens,[29] and increase of the mechanically loaded cross-section. However, for the dental attachment-based soldered framework specimens, no significant difference was determined between the unveneered and veneered framework specimens. The influence of the veneering process on the fracture strength of FDP has been frequently investigated in the literature with different and sometimes contradictory results, where a significant increase,[28,29] decrease,[30] or no influence at all were reported.[35]

In this study, the framework specimens were manufactured differently, but the veneering process was done uniformly. It therefore appears that for monolithic framework specimens, the positive effects of veneering outweigh the negative effects. For glass-soldered framework specimens, however, the negative influencing factors of the veneering process are increased. One explanation might be the varying CTEs of the materials used. During the veneering process, the different CTE can lead to the development of thermally induced residual stresses, reducing the fracture load. Nevertheless, the fracture load was not lower than for unveneered specimens and was in the range of the maximum reported biting forces.[34–36]

During dynamic tests, no clear differences were observed between the groups. Framework specimens of all groups survived 2 million cycles with a maximum load of 600 N. The remaining load bearing capacity of these specimens was still

in the range of the statically tested framework specimens. At higher loads, no differences were observed regarding the fracture pattern or survived cycles between the groups. Overall, the cycles until failure decreased with increasing dynamic load. To the best of the author's knowledge, no fatigue limit for clinical acceptance has yet been reported and therefore future studies should focus on comprehensive dynamic tests in clinical situations. The reported loads of this study can be used as the basis for future studies with the framework specimens. Within the extensive staircase tests as described in ISO 14801:2016,[26] 600 N could be used as a starting value.

Moreover, the results of the dynamic tests emphasize the feasibility of the glass-soldering technology for producing fatigue-resistant joints, as no differences with the monolithic framework specimens were apparent. To the best of the author's knowledge, no cyclic tests on soldered framework specimens have been carried out previously.

The observed fracture patterns in the connector region, lateral fracture of the tooth flanks and chipping of the veneer were similar to previous experimental findings.[17,22] However, for the diagonal joint geometry and the vertical joint geometry with an occlusal cap, some specimens fractured in the soldered joint. As described by Sass et al,[20] a high-quality standard of the joint is necessary to achieve a high bond strength. Air voids and misalignment of the subcomponents must be prevented and the joint surfaces must be homogeneously wetted with the glass solder. For all the framework specimens that fractured at the solder joint, the μCT scans showed manufacturing defects such as air voids or incorrect alignment of the subcomponents. The dental attachment-based joint geometry showed the most reproducible characteristics with respect to the quality of the glass-soldered joint and fracture strength.

The fracture of the framework at the second premolar was caused by two superimposed loads: first, the induced bending of the whole framework and secondly the contact loads around the tooth cusps. The applied contact condition at the second premolar forms compressive forces, which lead to the described subsurface cracking. Additionally, the tooth cusps are pressed apart and tensile stresses are formed pericoronally. This mechanical condition led to the splitting of the teeth. Furthermore, the connector region has the smallest cross-section and therefore the highest tensile stresses at the gingival side, which explains the fracture at this location.

As the fracture load is influenced by many factors including the test method (testing of untreated or altered specimens),[23,24,30,31,38–40] design and manufacturing of the framework,[11,21,23,28,41] the material and technique of the veneering process,[25,28–30,35] and the jaw model used,[42–44] the results of the present study are subject to some limitations.

The influence of the abutment material and teeth mobility on the fracture strength was comprehensively investigated. Due to the use of a stiff jaw model (Young´s modulus: ~70 GPa) and immobile abutment teeth, the static fracture load and the fatigue strength are probably overestimated.[42–44] Mahmood et al[44] have shown that especially the abutment material has a major impact on the fracture strength and

FRACTURE STRENGTH OF MONOLITHIC AND GLASS-SOLDERED CERAMIC SUBCOMPONENT

AMERICAN COLLEGE OF PROSTHODONTISTS
Your smile. Our specialty.®

| 9

modes. However, the observed fracture modes in the present study were comparable to other studies.[22,31,38,45] Therefore, it is assumed that the jaw model used is sufficient to study the general feasibility of the joining approach, however, future studies should focus on the fracture strength with more realistic jaw models.

Kohorst et al[24] summarized factors of the aging of zirconia-based FDP in the oral environment, which is caused by stress-corrosion at the crack tip, incorporation of water molecules in the zirconia lattice and tetragonal to monoclinic phase transformation. Within the present study, thermal or mechanical aging was not investigated and therefore should be addressed in future studies.

The veneering process of this study was done based on the instruction guidelines and by one experienced dental technician. A representative occlusal surface was generated in order to match the anatomic occlusal surface and to achieve a low variability between the groups. However, the thickness of the veneer layer and differences in the occlusal surfaces were not systematically controlled and an influence on the mechanical behavior of the framework specimens cannot be ruled out. Therefore, the influence of the veneering technique and layer thickness should be evaluated in further investigations.

Additionally, a small sample size was tested dynamically and the results must be statistically proven. Further studies are also necessary to evaluate the marginal fit of the long-span FDP and the overall clinical applicability of the glass-soldered subcomponents for long-span FDP.

Despite the aforementioned limitations of this study, the first null hypothesis was accepted, and it is therefore assumed that the investigated unveneered and veneered framework specimens have adequate strength to withstand acting biting forces.

The second null hypothesis was accepted. The mechanical strength of soldered framework specimens with different joining geometries was not significantly different. However, descriptive analysis showed the favorable alignment and soldering quality (lack of voids) of the framework specimens with a joint geometry based on a dental attachment.

CONCLUSION

Within the specified limitations, the defined null hypotheses were accepted. The glass-soldering technology proved the possibility of joining Y-TZP based subcomponents of 5-unit framework specimens with high fracture strength and fatigue resistance comparable to that of monolithic framework specimens. And the examined joining geometry did not influence the fracture strength of the soldered framework specimens.

However, further thermal treatments during veneering appears to have a negative effect on the fracture strength of soldered framework specimens, which should be investigated in detail in future studies. All groups have shown a static fracture strength greater than 1000 N, which was reported as a high biting force. In conclusion, soldering subcomponents of FDP might be feasible for clinical application; however,

further investigations are necessary to ensure a sufficient long-term survival rate.

CONFLICT OF INTEREST

The authors J.-O. Sass, U. Burmeister, H. Lang, R. Bader, and D. Vogel declare no conflict of interest.

C. Ganz and A. Mitrovic are employees of ZM Präzisionsdentaltechnik GmbH, Rostock, Germany, which are selling glass solders for joining ceramics in the field of dental technologies.

ORCID

Jan-Oliver Sass MSc https://orcid.org/0000-0003-4317-6025

REFERENCES

1. Chen Y-W, Moussi J, Drury JL, Wataha JC. Zirconia in biomedical applications. Expert Rev Med Devices. 2016;13:945–63.
2. Garvie RC, Hannink RH, Pascoe RT. Ceramic Steel? In: Sōmiya S, Moriyoshi Y (eds). Sintering Key Papers. Dordrecht: Springer Netherlands, 1990:253–7.
3. Nejatidanesh F, Abbasi M, Savabi G, Bonakdarchian M, Atash R, Savabi O, et al. Five year clinical outcomes of metal ceramic and zirconia-based implant-supported dental prostheses: A retrospective study. J Dent. 2020;100:103420.
4. Zarone F, Di Mauro MI, Spagnuolo G, Gherlone E, Sorrentino R, et al. Fourteen-year evaluation of posterior zirconia-based three-unit fixed dental prostheses: A Prospective clinical study of all ceramic prosthesis. J Dent. 2020;101:103419.
5. Limones A, Molinero-Mourelle P, Azevedo L, Romeo-Rubio M, Correia A, Gómez-Polo M, et al. Zirconia-ceramic versus metal-ceramic posterior multiunit tooth-supported fixed dental prostheses: A systematic review and meta-analysis of randomized controlled trials. J Am Dent Assoc. 2020;151:230–8.e7.
6. Elshahawy W, Watanabe I. Biocompatibility of dental alloys used in dental fixed prosthodontics. Tanta Dental Journal. 2014;11:150–9.
7. Haugli KH, Syverud M, Samuelsen JT. Ion release from three different dental alloys - effect of dynamic loading and toxicity of released elements. Biomater Investig Dent. 2020;7:71–9.
8. Sailer I, Strasding M, Valente NA, Zwahlen M, Liu S, Pjetursson BE, et al. A systematic review of the survival and complication rates of zirconia-ceramic and metal-ceramic multiple-unit fixed dental prostheses. Clin Oral Implants Res. 2018;29(Suppl 16):184–98.
9. Poggio CE, Ercoli C, Rispoli L, Maiorana C, et al. Metal-free materials for fixed prosthodontic restorations. Cochrane Database Syst Rev. 2017:CD009606.
10. Wittneben J-G, Buser D, Salvi GE, Bürgin W, Hicklin S, Brägger U, et al. Complication and failure rates with implant-supported fixed

10 | ACP AMERICAN COLLEGE OF PROSTHODONTISTS Your smile. Our specialty.®

SASS ET AL.

dental prostheses and single crowns: a 10-year retrospective study. Clin Implant Dent Relat Res. 2014;16:356–64.

11. Mahmood DJH, Linderoth EH, Steyern PV von, Wennerberg A: Fracture strength of all-ceramic (Y-TZP) three- and four-unit fixed dental prostheses with different connector design and production history. Swed Dent J. 2013;37:179–87.

12. Schmitter M, Mussotter K, Rammelsberg P, Gabbert O, Ohlmann B, et al. Clinical performance of long-span zirconia frameworks for fixed dental prostheses: 5-year results. J Oral Rehabil. 2012;39:552–7.

13. Denkena B, Breidenstein B, Busemann S, Lehr CM. Impact of hard machining on zirconia based ceramics for dental applications. Procedia CIRP. 2017;65:248–52.

14. Edwards Rezende CE, Sanches Borges AF, Macedo RM, Rubo JH, Griggs JA, et al. Dimensional changes from the sintering process and fit of Y-TZP copings: Micro-CT analysis. Dent Mater. 2017;33:e405–13.

15. Denry I, Kelly J. State of the art of zirconia for dental applications. Dent Mater. 2008;24:299–307.

16. Lee J-Y, Choi S-J, Kim M-S, Kim Ha-Y, Kim Y-S, Shin S-W, et al. Effect of span length on the fit of zirconia framework fabricated using CAD/CAM system. J Adv Prosthodont. 2013;5:118–25.

17. Wimmer T, Hostettler J Beuer F, Stawarczyk B. Load-bearing capacity of soldered and subsequently veneered 4-unit zirconia FDPs. J Mech Behav Biomed Mater. 2013;23:1–7.

18. Matsumoto W, Beraldo PP, De Almeida RP, Macedo AP, Kubata BR, Hotta TH, et al. Evaluation of marginal misfit of metal frameworks welded by gas-torch, laser, and tungsten inert gas methods. Int J Dent. 2018;2018:9828929. https://doi.org/10.1155/2018/9828929

19. Byrne G. Soldering in prosthodontics–an overview, part I. J Prosthodont. 2011;20:233–43.

20. Sass J-O, Jakobi A, Mitrovic A, Ganz C, Wilken J, Burmeister U, Lang H, Bader R, Vogel D, et al. Bending strength of ceramic compounds bonded with silicate-based glass solder. Materials Testing. 2021;63:593–8.

21. Larsson C, Holm L, Lã–Vgren N, Kokubo Y, Vult Von Steyern P, et al. Fracture strength of four-unit Y-TZP FPD cores designed with varying connector diameter. An in-vitro study. J Oral Rehabil. 2007;34:702–9.

22. Chai H, Lee JJ-W, Lawn BR. On the chipping and splitting of teeth. J Mech Behav Biomed Mater. 2011;4:315–21.

23. Beuer F, Steff B, Naumann M, Sorensen JA. Load-bearing capacity of all-ceramic three-unit fixed partial dentures with different computer-aided design (CAD)/computer-aided manufacturing (CAM) fabricated framework materials. Eur J Oral Sci. 2008;116:381–6.

24. Kohorst P, Dittmer MP, Borchers L, Stiesch-Scholz M. Influence of cyclic fatigue in water on the load-bearing capacity of dental bridges made of zirconia. Acta Biomater. 2008;4:1440–7.

25. López-Suárez C, Castillo-Oyagüe R, Rodrã-Guez-Alonso V, Lynch CD, Suárez-García M-A-J, et al. Fracture load of metal-ceramic, monolithic, and bi-layered zirconia-based posterior fixed dental prostheses after thermo-mechanical cycling. J Dent. 2018;73:97–104.

26. ISO 14801:2016 (en), Dentistry — Implants — Dynamic loading test for endosseous dental implants.

27. Quinn GD: NIST Recommended Practice Guide: Fractography of Ceramics and Glasses: National Institute of Standards and Technology, 2020.

28. Mahmood DJH, Linderoth EH, Wennerberg A. Vult Von Steyern P: Influence of core design, production technique, and material selection on fracture behavior of yttria-stabilized tetragonal zirconia polycrystal fixed dental prostheses produced using different multilayer techniques: split-file, over-pressing, and manually built-up veneers. Clin Cosmet Investig Dent. 2016;8:15–27.

29. Sundh A, Sjogren G. Fracture resistance of all-ceramic zirconia bridges with differing phase stabilizers and quality of sintering. Dent Mater. 2006;22:778–84.

30. Sundh A, Molin M, Sjögren G. Fracture resistance of yttrium oxide partially-stabilized zirconia all-ceramic bridges after veneering and mechanical fatigue testing. Dent Mater. 2005;21:476–82.

31. Güngör MB, Nemli SK, Bal BT, Tamam E, Yılmaz H, Aydın C, et al. Fracture resistance of monolithic and veneered all-ceramic four-unit posterior fixed dental prostheses after artificial aging. J Oral Sci. 2019;61:246–54.

32. Bakke M. Bite force and occlusion. Semin Orthod. 2006;12:120–6.

33. Padma S, Umesh S, Asokan S, Srinivas T. Bite force measurement based on fiber Bragg grating sensor. J Biomed Opt. 2017;22:1–6.

34. Cosme DC, Baldisserotto SM, SdA C, Shinkai RS. Bruxism and voluntary maximal bite force in young dentate adults. Int J Prosthodont. 2005;18:328–32.

35. Rodrã-Guez V, Castillo-Oyagüe R, López-Suárez C, Gonzalo E, Peláez J, Suárez-García M-A-J, et al. Fracture load before and after veneering zirconia posterior fixed dental prostheses. J Prosthodont. 2016;25:550–6.

36. Tinschert J, Natt G, Mautsch W, Augthun M, et al. Fracture resistance of lithium disilicate-, alumina-, and zirconia-based three-unit fixed partial dentures: a laboratory study. Int J Prosthodont. 2001;14:231–38.

37. Kosmac T, Oblak C, Jevnikar P, Funduk N, Marion L, et al. The effect of surface grinding and sandblasting on flexural strength and reliability of Y-TZP zirconia ceramic. Dent Mater. 1999;15:426–33.

38. Schultheis S, Strub JR, Gerds TA, Guess PC. Monolithic and bi-layer CAD/CAM lithium-disilicate versus metal-ceramic fixed dental prostheses: comparison of fracture loads and failure modes after fatigue. Clin Oral Investig. 2013;17:1407–13.

39. Rosentritt M, Behr M, Gebhard R, Handel G. Influence of stress simulation parameters on the fracture strength of all-ceramic fixed-partial dentures. Dent Mater. 2006;22:176–82.

40. Curtis AR, Wright AJ, Fleming GJP. The influence of simulated masticatory loading regimes on the bi-axial flexure strength and reliability of a Y-TZP dental ceramic. J Dent. 2006;34:317–25.

41. Bahat Z, Mahmood DJH. Vult Von Steyern P: Fracture strength of three-unit fixed partial denture cores (Y-TZP) with different connector dimension and design. Swed Dent J. 2009;33:149–59.

42. Wimmer T, Erdelt K-J, Eichberger M, Roos M, Edelhoff D, Stawarczyk B, et al. Influence of abutment model materials on the fracture loads of three-unit fixed dental prostheses. Dent Mater J. 2014;33:717–24.

43. Rosentritt M, Behr M, Scharnagl P, Handel G, et al. Influence of resilient support of abutment teeth on fracture resistance of all-ceramic fixed partial dentures: an in vitro study. Int J Prosthodont. 2011;24:465–8.

44. Mahmood DJH, Linderoth EH, Vult Von Steyern P. Vult Von Steyern P: The influence of support properties and complexity on fracture strength and fracture mode of all-ceramic fixed dental prostheses. Acta Odontol Scand. 2011;69:229–37.

45. Esquivel-Upshaw JF, Mehler A, Clark AE, Neal D, Anusavice KJ, et al. Fracture analysis of randomized implant-supported fixed dental prostheses. J Dent. 2014;42:1335–42.